# THE ELECTRO-ELASTIC FIELDS IN A FUNCTIONALLY GRADIENT PIEZOELECTRIC STRIP WITH AN INTERNAL ELECTRODE

**C.-D. Chen** *

*Department of Aerospace and Systems Engineering*
*Feng Chia University*
*Taichung, Taiwan*

**Y.-C. Chen C.-C. Chen**

*Microsystems Technology Center*
*Industrial Technology Research Institute South*
*Tainan, Taiwan*

## ABSTRACT

In this paper, the electro-elastic fields in a functionally gradient piezoelectric strip with an internal semi-infinite electrode are analyzed by using Fourier transform and Wiener-Hopf technique. The exact forms of asymptotic solutions and intensity factor and energy are obtained. The energy density criterion is proposed to study the fracture behavior near the electrode tip. The fracture initiation angle depends on the fracture resistance of the piezoelectric ceramic, bonding strength between piezoelectric and electrode, and the direction of least energy density factor $S$ inside the piezoceramic.

**Keywords:** FPGM, Piezoelectricity, Fracture mechanics, Energy density criterion.

## 1. INTRODUCTION

Piezoelectric ceramics have been recently used as actuators because of their high electro-elastic coupling behavior, quick response and large generative force. Among these piezoelectric actuators, one common type is that the piezoelectric and electrodes are arrayed in space. During operation, the high electro-elastic field concentration could occur around the tips of the internal electrodes. Failures such as crack or delamination have been observed at the electrode tips after the device is subjected cycling fatigue [1]. Some researchers have made efforts on the singular analyses of piezoelectric-electrode system [2-11]. These researches show that the electro-elastic fields near the electrode tip exhibit the classic square root singularity. By extending the fracture mechanics in elastic medium, the energy release rate and energy density factor have been proposed to predict the fracture at the electrode tip.

A practical approach to relax the stress gradient near the junction of two or more materials is the use of functionally gradient materials (FGMs). The mechanics of the FGMs arise with responding the increasing demands of the materials. To analyze the stress or deformation behavior of the FGMs, the mathematical functions, such as exponential law [12,13] and power law [14,15] are commonly used to idealize the spatial variation of the material properties.

Many researchers have made efforts on the fracture mechanics of FGMs [13,16]. These studies, including inplane and antiplane problems, show that the asymptotic behavior near the crack tip in FGM is the same as in homogeneous medium. By extending the concept of FGMs, the functionally piezoelectric gradient materials (FPGMs) are proposed in recent years. Some reports of crack problem in FGPMs can be found in the literatures [13,17-18]. To explain the fracture behavior, the energy release rate criterion for conventional isotropic material is extended to piezoelectric [19]. The total energy considered is not only the elastic energy, but also the electrostatic energy. Another criterion, the minimum energy density criterion, can also be found in the literature [13,17,20]. In this criterion, the crack initiation angle is assumed to be the direction of the local minimum energy density.

In this paper, the Fourier transform and Wiener-Hopf technique are applied to investigate a piezoelectric strip containing a semi-infinite electrode at the middle plane. Analytical solutions of intensity factor and energy density factor are obtained.

## 2. BASIC EQUATIONS

Consider a functionally gradient piezoelectric strip containing an internal semi-infinite electrode as shown in Fig. 1. If the piezoelectric is polarized along the $z$-direction and no inplane forces are present, the constitutive equations can be written as

$$\tau_{xz} = C_{44}\gamma_{xz} - e_{15}E_x \tag{1a}$$

$$\tau_{yz} = C_{44}\gamma_{yz} - e_{15}E_y \tag{1b}$$

$$D_x = e_{15}\gamma_{xz} + \varepsilon_{11}E_x \tag{1c}$$

$$D_y = e_{15}\gamma_{yz} + \varepsilon_{11}E_y \tag{1d}$$

* Corresponding author (cdchen@fcu.edu.tw)


DOI : 10.1017/jmech.2015.43
Copyright © 2015 The Society of Theoretical and Applied Mechanics, R.O.C.
https://doi.org/10.1017/jmech.2015.43 Published online by Cambridge University Press

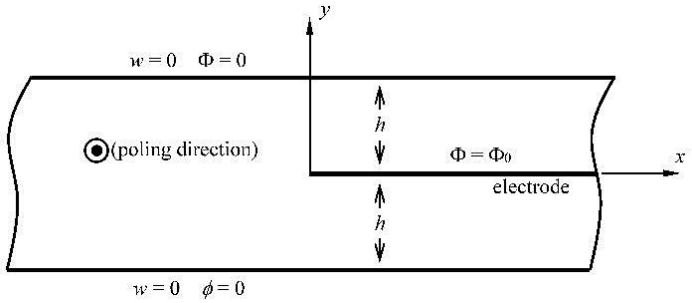



Fig. 1 A piezoelectric strip containing an internal semi-infinite electrode.

where $\tau_{xz}$, $\tau_{yz}$ are antiplane shear stresses, $D_x$, $D_y$ are inplane electric displacements, $\gamma_{xz}$, $\gamma_{yz}$ are shear strains, $E_x$, $E_y$ are electric fields, $C_{44}$ is elastic constant, $e_{15}$ is piezoelectric constant, and $\varepsilon_{11}$ is dielectric constant. The material properties of the piezoelectric are functions of $y$:

$$C_{44} = C_0 \exp[\alpha y] \tag{2a}$$

$$e_{15} = e_0 \exp[\alpha y] \tag{2b}$$

$$\varepsilon_{11} = \varepsilon_0 \exp[\alpha y] \tag{2c}$$

where $\alpha$ is the parameter of inhomogeneity, $C_0$, $e_0$ and $\varepsilon_0$ are the stiffness, piezoelectric constant and dielectric constant, respectively, when $y = 0$. The strain-displacement relations and equilibrium equations are

$$\gamma_{xz} = \frac{\partial w}{\partial x},\ \gamma_{yz} = \frac{\partial w}{\partial y},\ E_x = -\frac{\partial \Phi}{\partial x},\ E_y = -\frac{\partial \Phi}{\partial y} \tag{3}$$

$$\frac{\partial \tau_{xz}}{\partial x} + \frac{\partial \tau_{yz}}{\partial y} = 0,\ \frac{\partial D_x}{\partial x} + \frac{\partial D_y}{\partial y} = 0 \tag{4}$$

where $w$ and $\Phi$ are the antiplane displacement electric potential, respectively. Combination of Eqs. (1) ~ (4) yields

$$\left(\nabla^2 + \alpha \frac{\partial}{\partial y}\right) w = 0,\ \left(\nabla^2 + \alpha \frac{\partial}{\partial y}\right) \Phi = 0 \tag{5}$$

where $\nabla^2$ denotes the Laplacian operator.

## 3. STATEMENT OF PROBLEM

The functionally gradient piezoelectric strip is shown in Fig. 1. The boundary conditions at the top and bottom surfaces are

$$w(x, \pm h) = 0 \tag{6a}$$

$$\Phi(x, \pm h) = 0 \tag{6b}$$

The electrode is very thin such that its thickness is ignored and consequently, the present of the electrode does not affect the total stiffness of the piezoelectric strip. Because of the geometric symmetry, only the upper half, *i.e.* $y \geq 0$, is analyzed. The symmetric conditions at $y = 0$ are

$$\tau_{yz}(x, 0) = 0,\ -\infty < x < \infty \tag{7a}$$

$$D_y(x, 0) = 0,\ x > 0 \tag{7b}$$

$$\Phi(x, 0) = \Phi_0,\ x < 0 \tag{7c}$$

By the superposition principle, the solutions of the displacement and electric potential can be expressed as

$$w(x, y) = w^*(x, y) - \frac{e_0 \Phi_0}{C_0 (1 - e^{-\alpha h})}(e^{-\alpha y} - e^{-\alpha h}) \tag{8a}$$

$$\Phi(x, y) = \Phi^*(x, y) + \frac{\Phi_0}{1 - e^{-\alpha h}}(e^{-\alpha y} - e^{-\alpha h}) \tag{8b}$$

where $w^*$ and $\Phi^*$ are the solutions of the boundary value problem:

$$\left(\nabla^2 + \alpha \frac{\partial}{\partial y}\right) w^* = 0,\ \left(\nabla^2 + \alpha \frac{\partial}{\partial y}\right) \Phi^* = 0,\quad -\infty < x < \infty,\ 0 \leq y \leq h \tag{9}$$

$$w^*(x, h) = 0 \tag{10a}$$

$$\Phi^*(x, h) = 0 \tag{10b}$$

$$\tau^*_{yz}(x, 0) = 0,\ -\infty < x < \infty, \tag{10c}$$

$$D^*_y(x, 0) = D_0,\ x > 0 \tag{10d}$$

$$\Phi^*(x, 0) = 0,\ x < 0 \tag{10e}$$

with

$$\tau^*_{yz} = C_{44} \frac{\partial w^*}{\partial y} + e_{15} \frac{\partial \Phi^*}{\partial y} \tag{11a}$$

$$D^*_y = e_{15} \frac{\partial w^*}{\partial y} - \varepsilon_{15} \frac{\partial \Phi^*}{\partial y} \tag{11b}$$

$$D_0 = \alpha \left(\frac{e_0^2}{C_0} + \varepsilon_0\right) \frac{\Phi_0}{1 - e^{-\alpha h}} \tag{12}$$

## 4. THE FOURIER TRANSFORM AND WIENER-HOPF TECHNIQUE

The Fourier transform is defined as

$$\hat{f}(\xi, y) = \int_{-\infty}^{\infty} f(x, y)\, e^{ix\xi} d\xi \tag{13a}$$

The inverse transform is

$$f(x, y) = \frac{1}{2\pi} \int_{\Gamma} \hat{f}(\xi, y)\, e^{-ix\xi} d\xi \tag{13b}$$



https://doi.org/10.1017/jmech.2015.43 Published online by Cambridge University Press

where $\hat{f}(\xi, y)$ is the Fourier transform of $f(x, y)$, $\xi$, the Fourier transform parameter, is allowed to be complex number ($\xi = \sigma + i\tau$, $\sigma$ and $\tau$ are both real), $\Gamma$ denotes the inverse integral path.

Based on the Fourier transform, the general solutions of the differential Eq. (9) associated with the regular boundary conditions (10a), (10b) and (10c) can be expressed as

$$w^*(x,y) = \frac{1}{2\pi}\int_{\Gamma} A(\xi)\left[e^{\lambda_1 y} - e^{(\lambda_1-\lambda_2)h+\lambda_2 y}\right]e^{-ix\xi}d\xi \quad (14a)$$

$$\Phi^*(x,y) = -\frac{C_0}{e_0}w^*(x,y) \quad (14b)$$

where

$$\lambda_1 = \frac{-\alpha - (\alpha^2+4\xi^2)^{1/2}}{2} \quad (15a)$$

$$\lambda_1 = \frac{-\alpha + (\alpha^2+4\xi^2)^{1/2}}{2} \quad (15b)$$

Define

$$\hat{D}_+(\xi) = \int_0^{\infty} D_y^*(x,0)\, e^{ix\xi}dx \quad (16a)$$

$$\hat{\Phi}_-(\xi) = \int_{-\infty}^{0} \Phi^*(x,0)\, e^{ix\xi}dx \quad (16b)$$

then the Fourier transforms of $D_y(x, 0)$ and $\Phi(x, 0)$ are

$$\hat{D}_y^*(\xi,0) = \hat{D}_+(\xi) - \frac{D_0}{i\xi} \quad (17a)$$

$$\hat{\Phi}^*(\xi,0) = \hat{\Phi}_-(\xi) \quad (17b)$$

It can be shown that there exist two real numbers $\tau_+$ and $\tau_-$ such that $\hat{D}_+(\xi)$ and $\hat{\Phi}_-(\xi)$ are analytic in half planes $\tau > \tau_+$ and $\tau < \tau_-$, respectively. Combination of Eqs. (10d), (10e), (17a) and (17b) gives

$$\left(e_0 + \frac{C_0\varepsilon_0}{e_0}\right)\left[\lambda_1 - \lambda_2 e^{(\lambda_1-\lambda_2)h}\right]A(\xi) = \hat{D}_+(\xi) - \frac{D_0}{i\xi} \quad (18a)$$

$$-\frac{C_0}{e_0}\left[1 - e^{(\lambda_1-\lambda_2)h}\right]A(\xi) = \hat{\Phi}_-(\xi) \quad (18b)$$

Eliminating $A(\xi)$ in Eqs. (18a) and (18b) gives

$$\hat{D}_+(\xi) - \left(\varepsilon_0 + \frac{e_0^2}{C_0}\right)K(\xi)\,\hat{\Phi}_-(\xi) = \frac{D_0}{i\xi} \quad (19)$$

where the kernel $K(\xi)$ is

$$K(\xi) = \frac{\lambda_2 e^{\lambda_1 h} - \lambda_1 e^{\lambda_2 h}}{e^{\lambda_2 h} - e^{\lambda_1 h}} \quad (20)$$

Equation (19) is the Wiener-Hopf equation, which can be solved by a standard procedure. Let the kernel have the form

$$K(\xi) = K_+(\xi)K_-(\xi) \quad (21)$$

It can be shown that $K_+(\xi)$ and $K_-(\xi)$ are analytic in some upper and lower half planes, respectively. Substituting Eq. (21) into (19), we have

$$\frac{\hat{D}_+(\xi)}{K_+(\xi)} - \frac{D_0}{i\xi K_+(\xi)} = \left(\varepsilon_0 + \frac{e_0^2}{C_0}\right)K_-(\xi)\,\hat{\Phi}_-(\xi) \quad (22)$$

Introduce two functions $Q_+(\xi)$ and $Q_-(\xi)$ defined as

$$Q_+(\xi) = -\frac{D_0}{i\xi}\left(\frac{1}{K_+(\xi)} - \frac{1}{K_+(0)}\right) \quad (23a)$$

$$Q_-(\xi) = -\frac{D_0}{i\xi}\frac{1}{K_+(0)} \quad (23b)$$

Using Eqs. (23a) and (23b), Eq. (22) becomes

$$\frac{\hat{D}_+(\xi)}{K_+(\xi)} + Q_+(\xi) = \left(\varepsilon_0 + \frac{e_0^2}{C_0}\right)K_-(\xi)\Phi_-(\xi) - Q_-(\xi) \equiv E(\xi) \quad (24)$$

It can be shown that the left hand side of Eq. (24) is analytic in some upper plane, while the right hand side is analytic in some lower plane. The analytic continuation of Eq. (24) implies that $E(\xi)$ is an entire function. In order to find $E(\xi)$, $K_+(0)$ appeared in Eq. (23) and the asymptotic behavior of $K_+(\pm\infty)$, $K_-(\pm\infty)$ have to be investigated first.

Since the poles of $K(\xi)$ are $\pm i\,(n^2\pi^2/h^2 + \beta^2)^{1/2}$, there exists a positive real number $\tau_0 < (n^2\pi^2/h^2 + \beta^2)^{1/2}$ such that $K(\xi)$ is analytic in the strip $-\tau_0 < \tau < \tau_0$. Introduce a complex function $L(\xi)$ defined as

$$L(\xi) = \frac{K(\xi)}{(\xi - i\tau_0)^{1/2}(\xi + i\tau_0)^{1/2}} \quad (25)$$

By the Cauchy integral formula, $L(\xi)$ can be decomposed as

$$L(\xi) = L_+(\xi)L_-(\xi) \quad (26)$$

where

$$\ln L_+(\xi) = \frac{1}{2\pi i}\int_{i\tau_0-\infty}^{i\tau_0+\infty}\frac{\ln L(\zeta)}{\zeta - \xi}d\zeta \quad (27a)$$

$$\ln L_-(\xi) = -\frac{1}{2\pi i}\int_{-i\tau_0-\infty}^{-i\tau_0+\infty}\frac{\ln L(\zeta)}{\zeta - \xi}d\zeta \quad (27b)$$

From Eqs. (21), (25) and (26), it gives

$$K_+(\xi) = (-i)^{1/2}(\xi + i\tau_0)^{1/2}L_+(\xi) \quad (28a)$$



https://doi.org/10.1017/jmech.2015.43 Published online by Cambridge University Press

$$K_-(\xi) = i^{1/2}(\xi - i\tau_0)^{1/2} L_-(\xi) \tag{28b}$$

Since $L(\xi)$ is an even function, $L_+(0) = [L(0)]^{1/2}$. Then $K_+(0)$ can be obtained to be

$$K_+(0) = \left(\frac{\alpha}{1-e^{-\alpha h}}\right)^{1/2} \tag{29}$$

Next we shall investigate the asymptotic behavior of $K_+(\pm\infty)$ and $K_-(\pm\infty)$. From Eqs. (20) and (25), we know that

$$\lim_{\xi\to\pm\infty} L(\xi) = 1 \tag{30}$$

By the use of Eqs. (27) and (30), it gives

$$\lim_{\xi\to\pm\infty} L_+(\xi) = \lim_{\xi\to\pm\infty} L_-(\xi) = 1 \tag{31}$$

Then from Eqs. (28a) and (28b), the asymptotic behavior of $K_+(\pm\infty)$ and $K_-(\pm\infty)$ are

$$\lim_{\xi\to\pm\infty} K_+(\xi) \propto |\xi|^{1/2} \tag{32a}$$

$$\lim_{\xi\to\pm\infty} K_-(\xi) \propto |\xi|^{1/2} \tag{32b}$$

From Eqs. (24), (32) and the fact that

$$\lim_{\xi\to\pm\infty} \hat{D}_+(\xi) = \lim_{\xi\to\pm\infty} \hat{\Phi}_-(\xi) = 0 \tag{33}$$

it gives

$$\lim_{\xi\to\pm\infty} E(\xi) = 0 \tag{34}$$

Since $E(\xi)$ is an entire function, form Liouville theorem, we have

$$E(\xi) \equiv 0 \tag{35}$$

Substitution of Eq. (35) into (24) yields

$$A(\xi) = A_0 \frac{K_+(\xi)}{\xi(\lambda_2 e^{(\lambda_1-\lambda_2)h} - \lambda_1)} \tag{36}$$

From Eqs. (8a), (14a) and (36), the displacement field is

$$w(x,y) = \frac{A_0}{2\pi}\int_\Gamma K_+(\xi)\frac{e^{\lambda_1 y} - e^{(\lambda_1-\lambda_2)h+\lambda_2 y}}{\xi(\lambda_2 e^{(\lambda_1-\lambda_2)h} - \lambda_1)} e^{-ix\xi} d\xi - \frac{e_0\Phi_0}{C_0(1-e^{-\alpha h})}(e^{-\alpha y} - e^{-\alpha h}) \tag{37a}$$

The shear stresses and electric displacements are

$$\tau_{xz}(x, y) = 0 \tag{37b}$$

$$\tau_{yz}(x, y) = 0 \tag{37c}$$

$$D_x(x,y) = \frac{-iA_0 e^{\alpha y}}{2\pi}\left(e_0 + \frac{\varepsilon_0 C_0}{e_0}\right)\int_\Gamma K_+(\xi)\frac{e^{\lambda_1 y} - e^{(\lambda_1-\lambda_2)h+\lambda_2 y}}{\lambda_2 e^{(\lambda_1-\lambda_2)h} - \lambda_1} e^{-ix\xi} d\xi \tag{37d}$$

$$D_y(x,y) = \frac{A_0 e^{\alpha y}}{2\pi}\left(e_0 + \frac{\varepsilon_0 C_0}{e_0}\right)\int_\Gamma K_+(\xi)\frac{\lambda_1 e^{\lambda_1 y} - \lambda_2 e^{(\lambda_1-\lambda_2)h+\lambda_2 y}}{\xi(\lambda_2 e^{(\lambda_1-\lambda_2)h} - \lambda_1)} e^{-ix\xi} d\xi + D_0 \tag{37e}$$

The inverse integral path $\Gamma$ must lie in the analytic strip. For convenience, an equivalent integral path shown in Fig. 2 is chosen to calculate Eq. (37). Since the exact form of $K_+(\xi)$ remains unknown, the full field solution of electro-elastic fields can not be obtained. However, the field solutions near the electrode tip can be obtained by letting $\xi \to \infty$. The results are given as

$$D_x(x, y) = -\frac{iA_0}{2\sqrt{\pi}}\left(e_0 + \frac{\varepsilon_0 C_0}{e_0}\right)\left[\frac{i^{1/2}}{(y-ix)^{1/2}} + \frac{(-i)^{1/2}}{(y+ix)^{1/2}}\right] \tag{38a}$$

$$D_y(x, y) = \frac{A_0}{2\sqrt{\pi}}\left(e_0 + \frac{\varepsilon_0 C_0}{e_0}\right)\left[\frac{i^{1/2}}{(y-ix)^{1/2}} - \frac{(-i)^{1/2}}{(y+ix)^{1/2}}\right] \tag{38b}$$

Equation (38) are the near field solutions, *i.e.*, $x \to 0$ and $y \to 0$. For polar coordinate representation, the solutions are

$$D_x(r, \theta) = -\frac{\Phi_0}{\sqrt{2\pi r}}\left(\varepsilon_0 + \frac{e_0^2}{C_0}\right)\sqrt{\frac{2\alpha}{1-e^{-\alpha h}}}\sin(\theta/2) \tag{39a}$$

$$D_y(r, \theta) = \frac{\Phi_0}{\sqrt{2\pi r}}\left(\varepsilon_0 + \frac{e_0^2}{C_0}\right)\sqrt{\frac{2\alpha}{1-e^{-\alpha h}}}\cos(\theta/2) \tag{39b}$$

where $r = \sqrt{x^2 + y^2}$, $x = r\cos\theta$ and $y = r\sin\theta$.



https://doi.org/10.1017/jmech.2015.43 Published online by Cambridge University Press

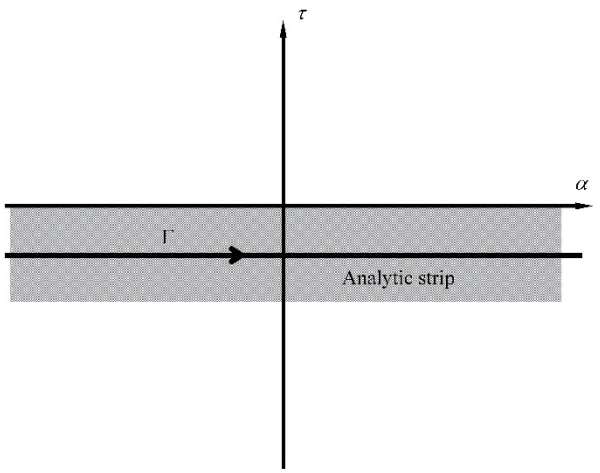



Fig. 2 An equivalent contour of inverse integral path $\Gamma$.

## 5. THE INTENSITY FACTOR AND ENERGY DENSITY CRITERION

From Eqs. (39a) and (39b), the electric displacement intensity factor $K_D$ is

$$K_D = \Phi_0 \left( \varepsilon_0 + \frac{e_0^2}{C_0} \right) \sqrt{\frac{2\alpha}{1-e^{-\alpha h}}} \tag{40}$$

Chen and Chue [7] studied the electrode in homogeneous piezoelectric strip. Eq. (40) can be reduced to Chen and Chue's results by letting $\alpha = 0$.

In this section, the energy density criterion is proposed to study the fracture behavior at the electrode tip. The energy density factor $S$ [20] is defined as

$$S = \lim_{r\to 0} r \frac{dW}{dV} = \lim_{r\to 0} \frac{r}{2} (\tau_{ij}\, \gamma_{ij} + D_i E_i) \tag{41}$$

Near the singularity point, $S$ can be expressed as function of $\theta$, *i.e.*, $S = S(\theta)$. The crack trends to initiate along the direction that the $S$ is local minimum denoted as $S_{\min}$. The rapid crack growth occurs when $S_{\min}$ reaches a critical value $S_c$.

By the definition, the energy density factor $S$ near the electrode tip can be obtained to be

$$S = \frac{\Phi_0^2}{2\pi} \left( \varepsilon_0 + \frac{e_0^2}{C_0} \right) \frac{\alpha}{1-e^{-\alpha h}} \tag{42}$$

For this case, $S$ is a constant and independent of $\theta$, that is, driving force that makes the crack propagation inside the piezoelectric is identical in every direction. Although the piezoelectric is inhomogeneous globally, the local region for $r \to 0$ can be considered as homogeneous. In such a small region, the material property $S_c^{(1)}$ to resist the crack propagation can be assumed to be identical in every direction. Denote that the bonding strengths between the two piezoelectric strips is $S_c^{(2)}$ and the bonding strength between the piezoelectric and electrode is $S_c^{(3)}$. By taking $S_c^{(1)}$, $S_c^{(2)}$ and $S_c^{(3)}$ into account simultaneously, we have three possible scenarios as the followings:

1. For the case that $S_c^{(1)}$ is the smallest, the crack will propagate along any direction inside the piezoelectric.
2. For the case that $S_c^{(2)}$ is smallest, debonding fracture will occur between the two piezoelectric strips, that is, the fracture initiation angle is along $\theta = 180°$.
3. For the case that $S_c^{(3)}$ is smallest, the electrode will delaminate from the piezoelectric, that is, the fracture initiation angle is along $\theta = 0°$.

The critical value of the electrical potential $(\Phi_0)_c$ is

$$(\Phi_0)_c = \sqrt{\frac{2\pi C_0 S_c}{C_0 \varepsilon_0 + e_0^2} \frac{1-e^{-\alpha h}}{\alpha}} \tag{43}$$

where the material property $S_c = \min[S_c^{(1)}, S_c^{(2)}, S_c^{(3)}]$.

## 6. CONCLUSIONS

In this paper, the coupling of antiplane deformation and inplane electric field of a functionally graded piezoelectric infinite strip with a semi-infinite electrode was investigated. The electric field near the electrode tip was found to exhibit square root singularity and the corresponding intensity factor was obtained in exact forms. The energy density criterion was proposed to study the fracture behavior near the electrode tip. The obtained energy density factor in the piezoelectric is a constant. Therefore, the fracture initiation angle depends on the fracture resistance of the piezoelectric ceramic, bonding strength between piezoelectric and electrode.

## ACKNOWLEDGEMENTS

This work is supported by the Ministry of Economic Affairs Taiwan through grant number D327JA1100.

## REFERENCES

1. Aburatani, H, Harada, S., Uchino, K., Furuta, A. and Fuda Y., "Destruction Mechanisms in Ceramic Multilayer Actuators," *Japanese Journal of Applied Physics*, **33**, pp. 3091–3094 (1994).
2. Shindo, Y., Narita, F. and Sosa, H., "Electroelastic Analysis of Piezoelectric Ceramics with Surface Electrodes," *International Journal of Engineering Science*, **36**, pp. 1001–1009 (1998).
3. He, L. H. and Ye, R. Q., "Concentration of Electric Field Near Electrodes on Piezoelectric Layer," *Theoretical Applied Fracture Mechanics*, **33**, pp. 101–106 (2000).
4. Ru, C. Q., "Exact Solution for Finite Electrode Layers Embedded at the Interface of Two Piezoelectric



https://doi.org/10.1017/jmech.2015.43 Published online by Cambridge University Press

Half-Planes," *Journal of the Mechanics and Physics of Solids*, **48**, pp. 693–708 (2000).
5. Li, X. F. and Duan, X. Y., "Electroelastic Analysis of a Piezoelectric Layer with Electrodes," *International Journal of Fracture*, **111**, pp. L73–L78 (2001).
6. Ye, R. Q. and He L. H., "Electric and Stresses Concentrations at the Edge of Parallel Electrodes in Piezoelectric Ceramics," *International Journal of Solids and Structures*, **38**, pp. 6941–6951 (2001).
7. Chen, C. D. and Chue, C. H., "Fracture Mechanics Analysis of a Composite Piezoelectric Strip with an Internal Semi-Infinite Electrode," *Theoretical and Applied Fracture Mechanics*, **39**, pp. 291–314 (2003).
8. Wang, B. L. and Mai Y. W., "An Electrode Analysis for Multilayer Ceramic Actuators," *Sensors and Actuators A*, **121**, 203–212 (2005).
9. Li, Y. D., Zhang, N and Lee, K. Y., "Effect of a Finite Interface on the Electrode in a Non-Homogeneous Piezoelectric Structure," *Smart Materials and Structures*, **18**, p. 125028 (2009).
10. Li, Y. D. and Lee K. Y., "Effects of Finite Dimension on the Electro-Elastic Responses of an Interface Electrode in a Piezoelectric Actuator," *Journal of Applied Mathematics and Mechanics*, **90**, pp. 42–52 (2010).
11. Wang, B. L., Han, J. C. and Du, S. Y., "Anti-Plane Mechanical and In-Plane Electrical Fields for a Finite Electrode/Punch on a Finite Piezoelectric Layer," *Fatigue & Fracture of Engineering Materials & Structures*, **34**, pp 139–148 (2011).
12. Delale F. and Erdogan F., "The Crack Problem for a Nonhomogeneous Plane," *Journal of Applied Mechanics*, **50**, pp. 609–614 (1983).
13. Chen, Y. J. and Chue, C. H., "Mode III Crack Problems of Two Bonded Functionally Graded Strips with Internal Cracks," *International Journal of Solids and Structures*, **46**, 331–343 (2009).
14. Lee, Y. D. and Erdogan, F., "Residual/Thermal Stress in FGM and Laminated Thermal Barrier Coatings," *International Journal of Fracture*, **69**, 145–165 (1995).
15. Reddy J. N., "Analysis of Functionally Graded Plates," *International Journal for Numerical Methods in Engineering*, **47**, 663–684 (2000).
16. Delale F. and Erdogan F., "On the Mechanical Modeling of the Interfacial Region in Bonded Half-Planes," *Journal of Applied Mechanics*, **55**, pp. 317–324 (1988)
17. Chue, C. H. and Ou, Y. L., "Mode III Crack Problems for Two Bonded Functionally Graded Piezoelectric Materials," *International Journal of Solids and Structures*, **42**, pp. 3321–3337 (2005).
18. Mousavi S. M. and Paavola J., "Analysis of Cracked Functionally Graded Piezoelectric Strip," *International Journal of Solids and Structures*, **50**, pp. 2449–2456 (2013).
19. Sosa H., "On the Fracture Mechanics of Piezoelectric Solids," *International Journal of Solids and Structures*, **29**, pp. 2613–1622 (1992).
20. Sih G. C., *Mechanics of Fracture Initiation and Propagation*, Kluwer Academic Publishers, Boston (1991).

(Manuscript received October 6, 2014,
accepted for publication January 21, 2015.)



https://doi.org/10.1017/jmech.2015.43 Published online by Cambridge University Press